Supporting information for

Ultrafast Plasmon-Enhanced Hot Electron Generation at Ag Nanocluster/Graphite Heterojunctions

Shijing Tan,[†] Liming Liu,[‡] Yanan Dai,[†] Jindong Ren,[†] Jin Zhao,[†,‡] Hrvoje Petek[*,†]

[†]Department of Physics and Astronomy and Pittsburgh Quantum Institute, University of Pittsburgh, Pittsburgh, PA 15260, USA

[‡]ICQD/Hefei National Laboratory for Physical Sciences at Microscale, and Key Laboratory of Strongly-Coupled Quantum Matter Physics, Chinese Academy of Sciences, and Department of Physics, University of Science and Technology of China, Hefei, Anhui 230026, China

[*]Corresponding author: petek@pitt.edu

1: The π-π* transition in Gr

In our recent multiphoton photoemission (mPP) spectroscopy study of the clean Gr surface with UV excitation we attributed the spectra to the π-π* transition superimposed on the thermionic emission background.[1] Here, we present the spectroscopy of the π-π* transition in more detail. The resonant π-π* transition takes place between the Dirac cones shown along at the M-K line in the Brillouin zone in Figure 1a. The electron population in π* band is expected to be excited in regions with high density-of-states (DOS), specifically, the saddle point in π* band near the M point and the von Hove singularity at ~1.5 eV above E_F [blue shaded rectangles in Figure 1a of the main text]. At these high DOS regions indirect excitations involving the simultaneous photon absorption and electron-phonon scattering are readily observed. Specifically, in 2PP spectra of HOPG with UV light, the first photon populates the π* band, and the second photon simultaneous with momentum scattering enables photoemission from the π* band to be observed in the normal emission.

As shown in Figure S1, in 2PP spectra with UV excitation (<400 nm) a broad, asymmetric, high-intensity peak appears near the work function edge, which is assigned to the indirect photoemission from the π* band.[2-3] We mark its energy at the position with highest intensity as shown by the black arrows in the inset of Figure S1a. Plotting the maximum energy position as a function of *hv* in Figure S1b gives a slope of 1.09 and an intercept of 1.46 eV, indicating that the 2PP process involves the population of an intermediate state in the vicinity of the von Hove singularity of the π* band,[4] which is detected by absorption of an additional photon.

Furthermore, the normalized spectra in Figure S1a show that the highest intensity of the π-π* feature is obtained with at 350 nm, i.e. hv=3.54 eV. This energy coincides with the 3.6 eV ⊥ -plasmon energy of Ag/Gr. Therefore, we expect strong coupling between the Mie plasmon and the

π-π* transition.

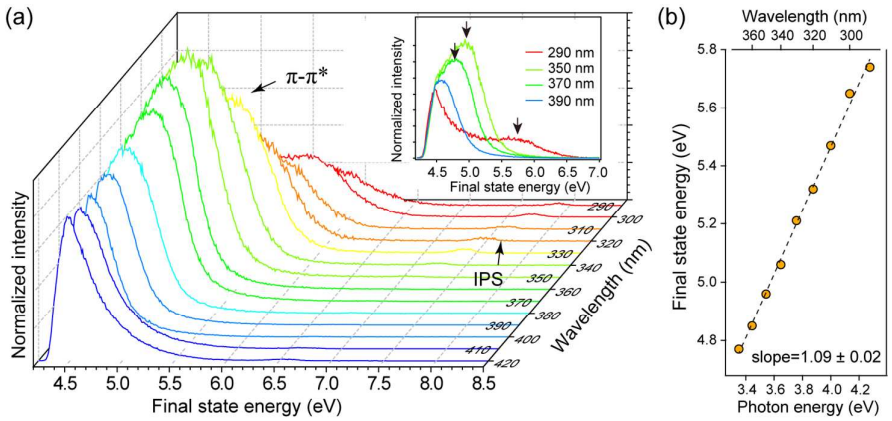

Figure S1. A series of 2PP spectra of pure HOPG with p-polarized excitation taken with *hv*=2.95-4.28 eV (420 to 290 nm). The inset shows the energy positions with highest intensity of the broad π-π* peak for selected 2PP spectra. (b) The plot of the energy of π-π* peak as a function of *hv* with hν≥3.35 eV.

2: The nonlinear order of photoemission for Ag/Gr surface

The calculation of the plasmon energy by comparing the normalized photoelectron yield at different *hv* assumes the *m*=2 power law dependence of the 2PP process. Thus, it is important to verify if the nonlinear photoemission from Ag/Gr with the *hv* range of 2.82-4.18 eV has the same order of 2. This concern arises from the unconventional nonlinear order for the clean graphite with VIS-IR excitation, where the exponent increases up to *m*=8 for IR excitation.[1] Here we confirm the nonlinear order for Ag/Gr by measuring the power dependence of the 2PP yield in the UV region. Two examples with *hv*=3.44 eV and *hv*=2.95 eV are shown in Figure S2a and S2b, respectively. The spectra show that photoelectrons are excited to a maximum final state energy of E_F+2*hv*, which also confirms the 2PP process. The integrated photoelectron yield, *Y*, of each spectrum is plotted as a function of laser fluence, *I*, in Figure S2c. The slope of the log-log plot gives the nonlinear order *m*, according to $Y \propto I^m$. The results in Figure S2c confirm the exponent *m*=2 for both *hv*=3.44 and 2.95 eV with p-

and s-polarization.

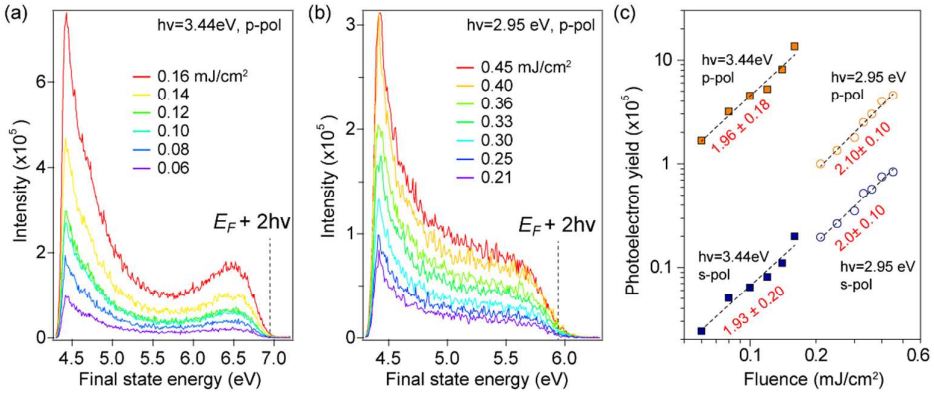

Figure S2. (a), (b) Power dependent 2PP spectra of Ag/Gr surface with p-polarized *hv*=3.44 and 2.95 eV excitation. (c) Log-log plots of photoelectron yields *vs.* the laser fluence. The numbers in red give the slope of each plot.

3: 2PP measurement at the Mo sample holder.

As discussed in the main text, the 2PP at the polycrystalline Mo sample holder is used to normalize the fluence, *I*, for different *hv*. Representative 2PP spectra at Mo sample holder with *hv*=3.44 eV in Figure S3a show no distinct spectral structures. Figure S3b gives the 2PP yield from the Mo sample holder as a function of *hv*. Although the fluence at each *hv* cannot be measured exactly, the photoemission yield ratio between the p- and s-polarized excitation gives a nearly constant value of ~2 (right axis in Figure S3b). This is in sharp contrast to the p/s ratio measured for the Ag/Gr surface in the Figure 3a of the main text, which characterizes the plasmonic enhancement factor for Ag/Gr.

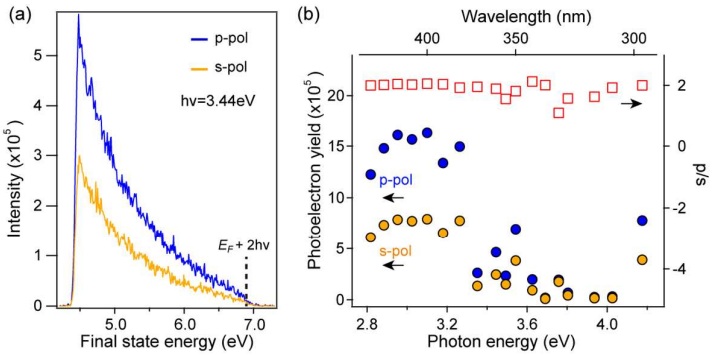

Figure S3. (a) 2PP spectra at Mo sample holder with *hv*=3.44 eV. (b) Plot of the photoemission yield with p- and s-polarized excitation (left axis) and their ratio (rectangles, right axis) *vs.* photon energy for the Mo sample holder.

4: 1PP spectra of the clean Gr and Ag/Gr surfaces

We measure one photon photoemission (1PP) to confirm the observation of the IFS in 2PP spectra. The clean Gr and Ag/Gr surfaces have approximate work functions of ~4.5 eV. When the *hv* energy exceeds the work function, 1PP dominates. Figure S4a shows the transition from 2PP to 1PP for the clean Gr when the photoexcitation *hv* is tuned from 3.82 to 5.06 eV. The contribution from the π-π* excitation to 2PP spectra becomes less prominant as the *hv* increases. When the *hv*>4.6 eV, 1PP from the occupied π-bands dominates the spectra, as seen in the inset. The photoemission at the threshold occurs from the occupied states near the K points where the π-bands cross the Fermi level. The signal can be observed at the Γ point through phonon-mediated scattering, as in the case of the π*-band in 2PP spectra. The 1PP spectra have a waning signal from work function edge to E_F, which probably reflects the change in the DOS of the π band near E_F. Figure S4b shows the 2PP and 1PP spectra for Ag/Gr. We expect the 1PP spectra of Ag/Gr to include contributions from both the π band, as the clean Gr surface, and the occupied IFS that is introduced by Ag chemisorption. To distinguish these two contributions, in Figures S4c and S4d we compared the 1PP spectra of the clean Gr and Ag/Gr with *hv*=4.60 and 5.06 eV, respectively. With *hv*=4.60 eV excitation, the photon energy is insufficient to excite photoemission from the occupied IFS, so the spectra of the clean Gr and Ag/Gr

are nearly identical; both are dominated by the π-band. By contrast, with *hv*=5.06 eV excitation, the 1PP spectra of Ag/Gr in Figure S4d show an additional contribution emanating from ~0.2 eV below the E_F, which is superposed on the π-band signal (red arrow in Figure S4d), which we attribute to 1PP from the occupied IFS based on its energy and association with the Ag nanocluster chemisorption. Note that although the IFS signal appears relatively strong compared to the DOS at E_F, its emission is allowed, whereas that for the π-band is phonon assisted. Moreover, the DOS of the π-band is minimum at E_F.

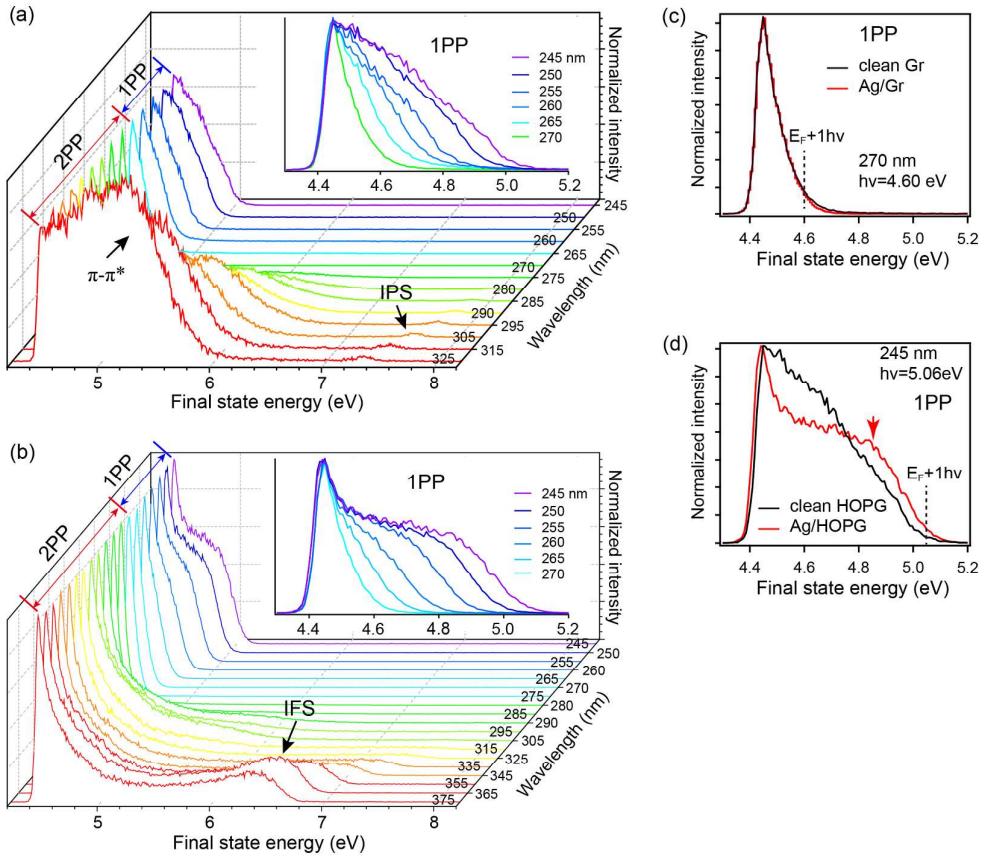

Figure S4: (a) A series normalized spectra of the clean Gr surface with p-polarized light for excitation with *hv*=3.82-5.06 eV (325 to 245 nm). With *hv*>4.5 eV, the spectra are excited by one photon process. The 1PP spectra are enlarged in the inset. (b) A series normalized spectra of Ag/Gr surface with p-polarized light for excitation with *hv*=3.31-5.06 eV (375 to 245 nm). (c), (d) 1PP spectra of the clean Gr and Ag/Gr excited by *hv*=4.60 eV and *hv*=5.06 eV, respectively. The red arrow in (d) indicates the IFS contribution at 0.2 eV below the E_F.

5: DFT calculation details

The electronic structure of Ag/Gr is calculated for three structure models: (1) a silver trimer cluster (Ag_3) on ten layers of Gr substrate; (2) Ag monolayer on three layers of Gr substrate; and (3) Ag bilayer on three layers of Gr substrate. The electronic structure calculation are performed using the VASP package[5-7] with PBE functional[8]. For the Ag_3 cluster calculations, the Gr layer distance is optimized to be 3.23 Å with the variance in the range of ±0.04 Å. Ag atoms are located at approximately on-top positions above C atoms of single C atom hexagons. In the geometry optimization and electronic self-consistent processes, the energy cutoffs for the plane wave basis are 400 and 800 eV, respectively. The k-mesh sampling of 9×9×1 and 5×5×1 were adopted for ten layers and three layers Gr models separately. The convergence criteria for the geometric optimization iterations is that the force on each atom should be less than 0.02 eV/Å, while for the electronic self-consistency iterations is that the total energy difference should be less than 1×10^{-5} eV. The vdW-D2[9] method is adopted to account for the dispersive interaction between the graphene layers.

Ag_3 on graphite retains its triangular configuration with the Ag-Ag bonds being stretched to 2.78 Å compared with its configuration in vacuum, as shown in Figure S5. The distance between Ag and closest C atom is 3.04 Å on average. The calculated adsorption energy is -0.23 eV and the Bader charge[10] loss from Ag_3 to Gr is 0.15 electron, or 0.05 electron/atom.

The calculations for the Ag monolayer and bilayer use a 5×5 surface unit cell of Ag on a 6×6 Gr substrate with 3 layer thickness, for which there is a lattice mismatch of -2.13% (Figure S6b and S6c). The Ag-Ag and Ag-C bond lengths are 2.95 and 3.12 Å. The calculated adsorption energy is -6.14 eV/supercell for the Ag monolayer and -6.82 eV/supercell for the Ag bilayer. The calculated PDOS shows both Ag monolayer and bilayer at Gr have the similar occupied states at ~0.2 eV below

E_F (Figure S6a). The spatial distribution of this occupied state shows the delocalized charge distribution at the interface (Figures S6d and S6e). Bader analysis shows the charge transfer from Ag to Gr is 0.24 electron/supercell for the monolayer and 0.50 electron/supercell for the bilayer.

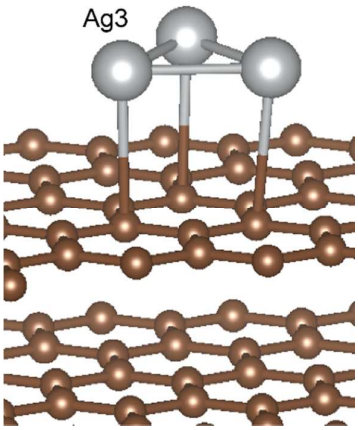

Figure S5. The structure model of Ag_3 on Gr.

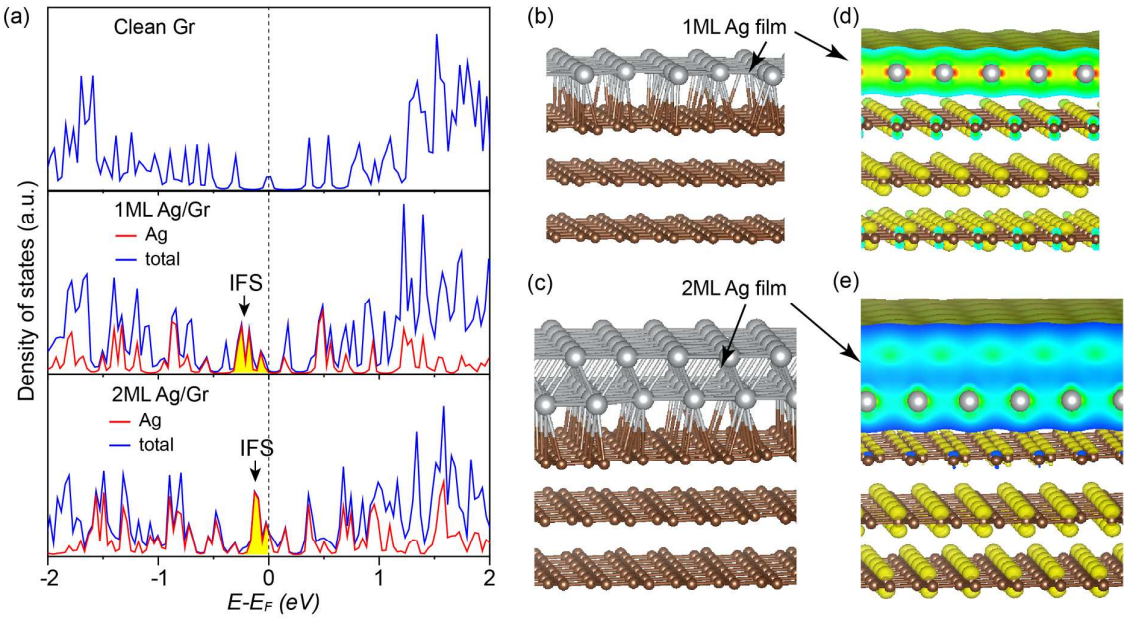

Figure S6. (a) The calculated PDOS of the clean Gr, monolayer Ag/Gr and bilayer Ag/Gr. The yellow shaded areas highlight the occupied IFS. (b), (c) The structure model of the monolayer Ag/Gr and bilayer Ag/Gr. (d), (e) The spatial distributions of the IFS for the monolayer Ag/Gr and bilayer Ag/Gr interfaces.

Reference:

1. Tan, S.; Argondizzo, A.; Wang, C.; Cui, X.; Petek, H., *Phys. Rev. X* **2017,** *7*, 011004.
2. Shibuta, M.; Yamamoto, K.; Miyakubo, K.; Yamada, T.; Munakata, T., *Phys. Rev. B* **2010,** *81*, 115426.
3. Pagliara, S.; Montagnese, M.; Dal Conte, S.; Galimberti, G.; Ferrini, G.; Parmigiani, F., *Phys. Rev. B* **2013,** *87*, 045427.
4. Moos, G.; Gahl, C.; Fasel, R.; Wolf, M.; Hertel, T., *Phys. Rev. Lett.* **2001,** *87*, 267402.
5. Kresse, G.; Hafner, J., *Phys. Rev. B* **1993,** *48*, 13115.
6. Kresse, G.; Hafner, J., *Phys. Rev. B* **1993,** *47*, 558.
7. Kresse, G.; Hafner, J., *Phys. Rev. B* **1994,** *49*, 14251.
8. Perdew, J. P.; Burke, K.; Ernzerhof, M., *Phys. Rev. Lett.* **1996,** *77*, 3865.
9. Grimme, S., *J. Comput. Chem.* **2006,** *27*, 1787.
10. Henkelman, G.; Arnaldsson, A.; Jonsson, H., *Comp. Mater. Sci.* **2006,** *36*, 354.